Nondestructive Identification of Internally Damaged Areas of Concrete Beam Using the Spectral Analysis of Surface Waves Method

M. E. KALINSKI, K. H. STOKOE II, J. O. JIRSA, AND J. M. ROESSET

An unidentified vehicle struck the bottom of a railroad overpass in Austin, Texas, and severely damaged one of the concrete beams in the overpass structure. The damaged beam was removed and taken intact to the University of Texas at Austin where the spectral analysis of surface waves (SASW) method was used to delineate nondestructively the damaged zones. SASW measurements performed on the overpass beam revealed a significant velocity contrast between damaged and undamaged zones. Damaged zones exhibited velocities ranging from 4,000 to 6,900 ft/sec (1,200 to 2,100 m/sec), depending on the extent of cracking. Velocities of undamaged zones ranged from 7,100 to 9,000 ft/sec (2,150 to 2,750 m/sec), with most values around 7,800 ft/sec (2,400 m/sec). The measurements were consistent with visual inspection of the beam. More important, the measurements indicated the presence of cracking that was not visually detectable.

A prestressed concrete beam in service on a railroad overpass bridge in Austin, Texas, was struck and severely damaged by an unidentified vehicle. The vehicle struck the side of the beam about 3 in. (8 cm) from its base. The beam was subsequently removed and taken intact to the University of Texas at Austin where researchers began testing the beam. The beam is 40-ft (12.2-m) long and constructed with concrete, possessing a reported 28-day compressive strength of 6,400 psi (44.1 MPa). Approximate dimensions of the beam are given in Figure 1. The inset in Figure 1 shows the location of the beam in the overpass structure and the impact area.

The objective of the work presented in this paper was to evaluate, nondestructively and noninvasively, the integrity (damaged versus undamaged zones) of the damaged overpass beam. This work represents an initial step in a comprehensive study of the load-carrying capacity of the beam, first in its damaged state and then after repair with an epoxy grout. Integrity testing of the damaged beam was conducted by applying the spectral analysis of surface waves (SASW) method. The SASW method measures surface wave velocities, which can be related to the properties of the material being tested. The main benefit of the SASW method is that information about interior profiles in beams can be obtained by making nondestructive measurements on only one side of the beam. Other nondestructive techniques from which comparable profiles can be developed, such as tomographic imaging with sonic waves, require access to both sides of the beam.

In this paper, a brief overview of the SASW method and its applications to this particular study are outlined. SASW results from the beam are then presented and compared with cracking patterns observed on the beam. Finally, the capabilities and limitations of the SASW method to detect cracks in structural concrete elements are discussed.

Department of Civil Engineering, University of Texas at Austin, Austin, Tex. 78712.

OVERVIEW OF SASW METHOD

Surface wave velocity measurements are one means of nondestructively obtaining information about the geometry and in-place elastic moduli of layered systems, such as geotechnical profiles and pavement systems (*1–3*). The SASW method provides a convenient approach to the measurement and analysis of surface wave velocities (*4–8*). When modulus varies with depth in a layered system, surface waves with different wavelengths travel at different velocities and are said to be dispersive. It is this dispersive characteristic that is measured in SASW testing.

Surface Wave Dispersion

How surface wave dispersion is measured in SASW testing is best explained by the example shown in Figure 2(a). Surface waves with frequencies f_1 and f_2 are seen to propagate through two different layered systems. The first system is a uniform half-space of intact concrete. The second system has a layer of intact concrete over damaged concrete. Relative vertical particle motion is shown as a function of depth for each surface wave. The motion represents the zone stressed (sampled) by each surface wave. The high-frequency wave, f_1, represents a short-wavelength wave and travels through shallow material. The velocity of the short-wavelength wave is a function of the near-surface elastic moduli, which, for the case shown, is 5,650 ksi (38.9 GPa) for both profiles. However, the lower-frequency wave, f_2, has a longer wavelength and travels through deeper material. Its velocity depends on the moduli of the near surface and deeper materials. Figure 2(b) shows the dispersion curves, plots of surface wave velocity versus wavelength, for each of the two systems in Figure 2(a) and illustrates how a dispersion curve can reveal the presence of a low-modulus layer beneath a high-modulus layer.

Measurement of Surface Wave Dispersion

SASW testing is performed with an energy source, two or more receivers, and recording instrumentation. The source and receivers are placed on the surface of a layered system along an array axis as

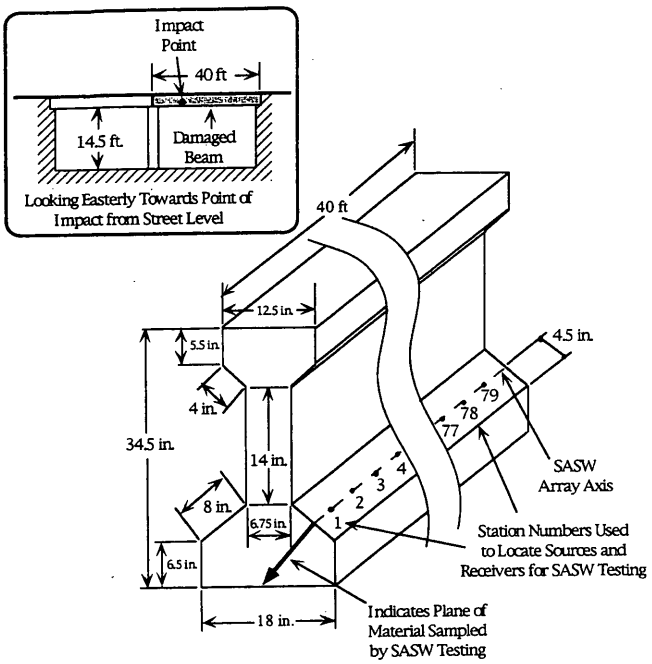

FIGURE 1 Approximate dimensions of prestressed concrete beam and locations where SASW testing was performed.

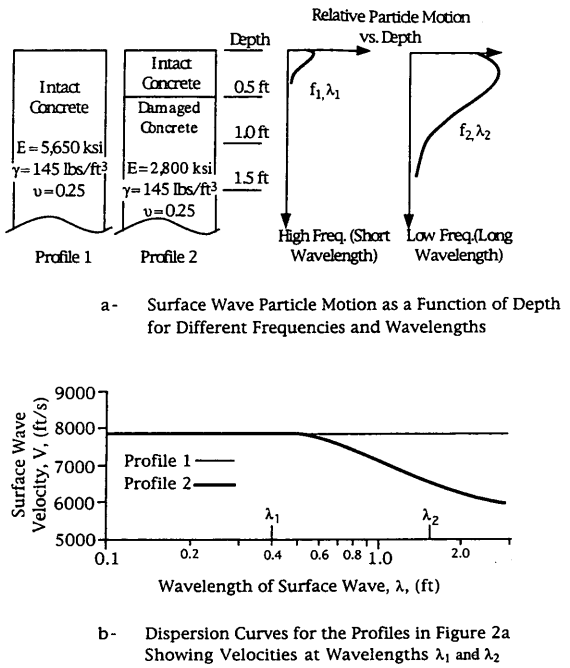

FIGURE 2 Effect of modulus variations on dispersion curve measured by the SASW method for two-layered systems.

shown in Figure 3. The source is used to impart energy to the surface vertically. Vertical motion at the two receiver locations is recorded in the time domain as transducer voltage, as shown in Figure 4(a). An exponential window typically is applied to the time records to attenuate later-arriving reflected energy relative to the direct arrival surface wave energy as shown in Figure 4(b) (*9*). The two windowed time-domain records, $x(t)$ and $y(t)$, are then converted to complex numbers, $X(f)$ and $Y(f)$, in the frequency domain using Fourier analysis. The cross power spectrum, $G(f)$, is defined as

$$G(f) = X(f)Y*(f) \tag{1}$$

where $Y*(f)$ is the complex conjugate of $Y(f)$. The phase of the cross power spectrum, $\Phi(f)$, is the phase difference between $X(f)$ and $Y(f)$ and is expressed as a function of frequency as follows:

$$\Phi(f) = \tan^{-1}\left\{\frac{Tm\,[G(f)]}{\mathrm{Re}\,[G(f)]}\right\} \tag{2}$$

The phase difference physically represents the number of cycles of a given frequency between two receiver locations as the waveform passes from one receiver to another. Relative, or "wrapped," phase differences fall between π and $-\pi$ radians as the phase values repeat themselves every 2π radians. The absolute number of cycles between receivers is determined by unwrapping the phase spectrum. Examples of wrapped and unwrapped phase spectra are shown in Figure 5(a). Once the phase spectrum is unwrapped, surface wave velocity, $V(f)$, can be calculated as a function of frequency as follows:

$$V(f) = \frac{2\pi \mathbf{R} f}{\Phi(f)} \tag{3}$$

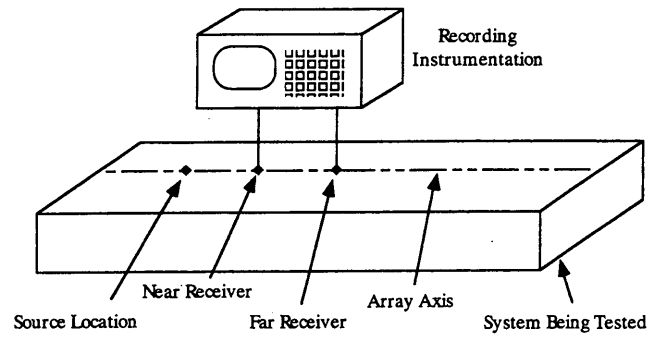

FIGURE 3 Typical SASW data acquisition setup.

where **R** is the receiver spacing, and $\Phi(f)$ is expressed in radians. Because velocity is the product of wavelength and frequency, the wavelength 1 associated with each frequency is simply

$$\lambda = \frac{2\pi \mathbf{R}}{\Phi(f)} \tag{4}$$

A dispersion curve of wave velocity versus wavelength is then constructed from all available frequencies using Equations 3 and 4. Development of a dispersion curve is the end-product of the physical measurement. Analytical modeling of the dispersion curve is performed subsequently to construct stiffness profiles (*10,11*).

Given a distance R between SASW array elements, velocities of wavelengths greater than $2R$ should not be considered valid because of near-field effects (*8,12*). For data acquisition on concrete or other

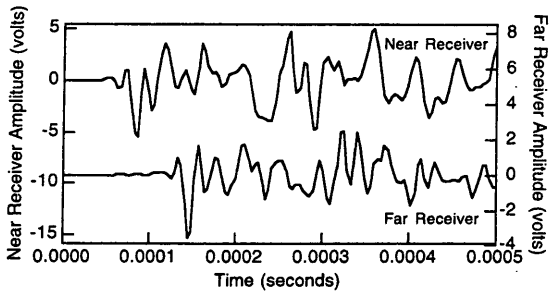

a- Unwindowed Time Records

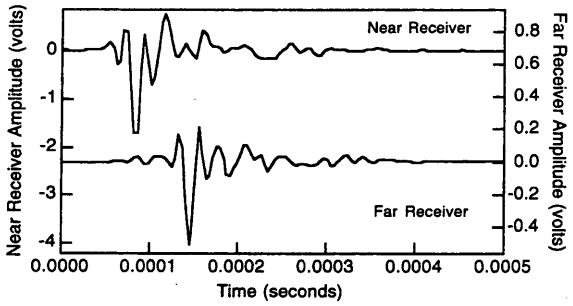

b- Windowed Time Records

FIGURE 4 Windowed and unwindowed time records recorded for SASW array 10–11.

systems possessing a finite thickness, the maximum recordable wavelength is constrained further by the thickness of the concrete. Velocity information for wavelengths greater than the thickness of the concrete is not valid because of interference from the other side of the concrete member.

APPLICATION OF SASW METHOD

Whereas the SASW method historically has been applied to describe layered systems, such as soil profiles and pavement systems, recent efforts have been made to apply the SASW method to the identification of cracking in concrete structural elements. Experimental and analytical work on rock, cracked concrete blocks, and prototype concrete structural elements has indicated that surface wave velocities decrease at all wavelengths when an open crack exists between the SASW receivers (*12,13*). In some cases, surface wave velocities measured in damaged concrete decreased without the presence of visible cracking between the receivers. This illustrates the potential of the SASW method to detect damage that is otherwise visually undetectable. However, surface wave velocities did not decrease when the receivers and the cracks were on opposite sides of the specimen and the crack depth was less than half of the specimen thickness. Surface wave velocities also have been observed to decrease in intact specimens at wavelengths greater than the thickness of the specimen because of interference from the other side of the specimen (*12,14*).

The damaged railroad overpass beam described in this paper provided an excellent opportunity to extend previous observations on cracked rock and concrete to an actual field-damaged specimen. SASW tests were performed on the side of the overpass beam that was struck. Source and receiver locations were designated as stations along an array axis, as shown in Figure 1. Stations were spaced 6 in. (15.2 cm) apart and were numbered 1 to 79. Figure 1 also shows the material being sampled beneath the array axis, as represented by the line extending from the array axis into the concrete along a plane perpendicular to the surface of the concrete beam.

SASW data were recorded using each pair of adjacent station locations as receiver locations. Dispersion curves were then determined for each of the receiver pairs. The dispersion curves were used to construct a mosaic of wave velocity versus depth into the beam by plotting dispersion curves along the length of the beam midway between the receiver locations used to determine each particular dispersion curve. For example, for the dispersion curve determined with the source at Station 9, a near receiver at Station 10 and a far receiver at Station 11, the dispersion curve was plotted at Station 10.5. To plot wave velocity versus depth, dispersion curves were smoothed and velocities were reported at 0.1-ft (0.03-m) wavelength intervals from 0.1 to 1.0 ft (0.03 to 0.3 m). Thus, a grid of velocity versus depth data was posted at 6-in. (15.2-cm) intervals along the beam and generated at 0.1-ft (3-cm) wavelength intervals into the beam. In this case, wavelength was approximated as depth into the beam.

Finally, velocity profiles at all mid-stations (such as Station 10.5 noted above) were contoured and compared with visual cracking

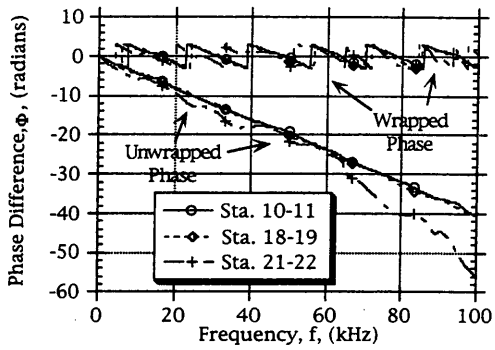

a- Cross Power Spectra

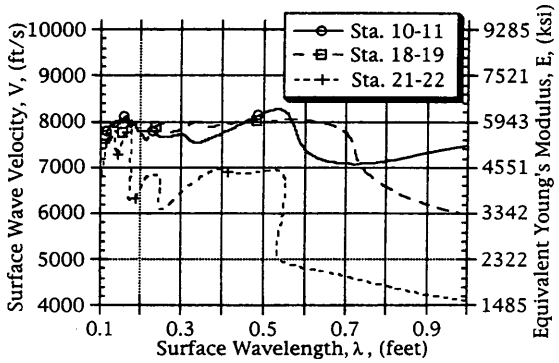

b- Dispersion Curves

FIGURE 5 Cross power spectra and dispersion curves for SASW Arrays 10–11, 18–19, and 21–22.

patterns to evaluate the ability of the method to identify and delineate cracked zones. Interpretations were made of the internal cracking pattern in the beam from observations made on all sides of the beam. The observations could be interpolated into the beam and cross-sections of the beam could be sketched showing the interpreted areas of internal damage at various positions. By comparing these cross-sections with the velocity profile, the SASW method was evaluated as a potential means of nondestructively identifying internal damage within the beam.

Note that the surface wave velocity of a given wavelength is not the velocity of the material at the depth equal to the wavelength. The velocity of a given wavelength depends on the velocity of all the material between the surface and about one wavelength in depth. Forward modeling or inversion is required to convert a dispersion curve into a profile of shear wave velocity or elastic modulus versus depth (*10*). However, previous experience indicates that dispersion curves can yield qualitative information about the internal condition of concrete, so dispersion curves were considered adequate to describe the concrete for this study.

RESULTS

Figure 6 shows each side of the beam, illustrating the observed cracking and the station locations used in SASW testing. Severely damaged and spalled zones are indicated by stippling, and the area of the impact is indicated with a large black dot. Three major systems of cracks existed in the beam. The first system is a group of concentric cracks on the impacted side of the beam. These cracks appear to be a direct result of the impact. The second system is a large cuspate delamination-type feature that expresses itself on the nonimpacted and bottom sides. The feature is concave toward the nonimpacted and bottom sides. The damage is characterized by a

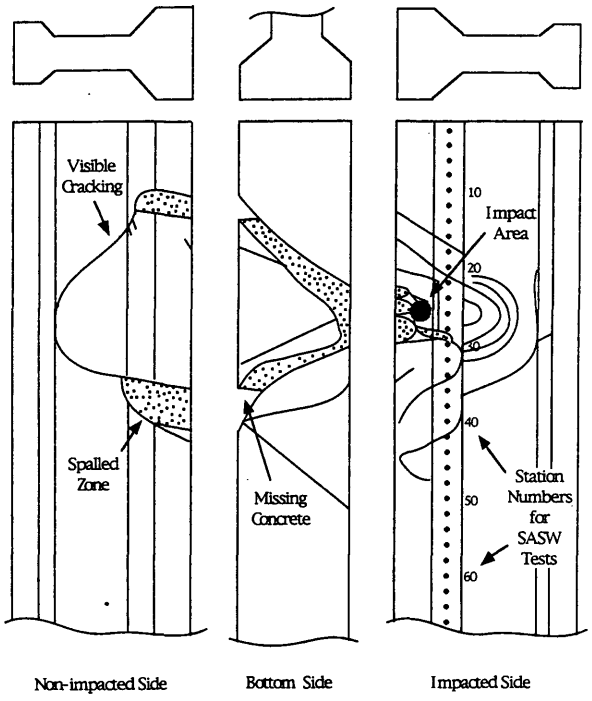

FIGURE 6 Visible cracking and spalling observed on each side of the overpass beam.

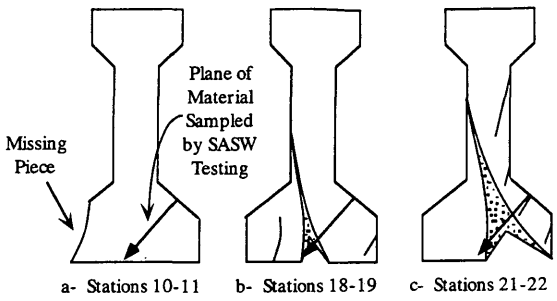

FIGURE 7 Cross sections along the beam showing interpreted areas of internal damage.

thick zone of highly fractured and spalling concrete where the zone intersects the surface of the beam. The feature appears to be a result of beam bending upon impact. It also appears to have permanently separated the cuspate section of concrete relative to the rest of the beam as a result of inelastic deformation of the prestressing tendons. The third system is cracking on the other side of the diaphragm from the impact area. The beam was attached to five other beams in the overpass structure, with a diaphragm near the center of each beam (between Stations 35 and 40 used in the SASW tests). When the impact occurred, the diaphragm acted as a reaction point on the beam and caused the beam to bulge outward. Cracks associated with the mechanism are not as well defined as the other two systems of cracks, but they seem to be present on the bottom and impact sides.

The first step to evaluating the success of the SASW method was to interpret the internal damage by observing cracking on the exterior of the beam. Cross-sections revealing the beam's internal damage were made at discrete intervals along the beam. Examples of these cross-sections are shown in Figure 7 for cross-sections between Stations 10 and 11, 18 and 19, and 21 and 22. These three cross-sections represent zones with varying degrees of visible damage on the side of the beam being tested. The cuspate damage system could be interpreted with relative confidence because it expressed itself on more than one side of the beam, but the other two systems only expressed themselves on one side of the beam, but the other two systems only expressed themselves on one side of the beam, so interpretations concerning them are not as reliable. Finally, SASW data were recorded for comparison with the cross sections.

Figure 4 shows a pair of unwindowed and windowed time records for SASW data recorded with Stations 10 and 11 as receiver locations. The records represent typical data obtained from an undamaged zone and show the attenuation of later-arriving energy relative to direct surface wave arrivals through the use of windowing.

Figure 5(a) shows the wrapped and unwrapped phase plots of the cross power spectra for data recorded between Stations 10 and 11, 18 and 19, and 21 and 22. Figure 5(b) shows the resulting dispersion curves calculated from these three phase spectra. The dispersion curves also indicate values for the equivalent Young's moduli. The equivalent moduli are based on assumptions of a concrete unit weight of 145 lb/ft^3 (2 330 kg/m^3), a Poisson's ratio of 0.25, and a reasonable thickness of similar material. The approximate relationship between surface wave velocity, V, and equivalent Young's Modulus, E, can then be given as follows (*15*):

$$E \cong 13.37\, V^2 \tag{5}$$

where V is in ft/sec, and E is in lb/ft^2.

The reasonably linear nature of the spectra in Figure 5(b) from the Station 10–11 array indicates a relatively uniform velocity within the concrete. Variations in velocity normally would express themselves as changes in slope of the unwrapped cross power spectra. However, the unwrapped phase is quite linear [Figure 5(a)]. The corresponding dispersion curve exhibits a relatively constant velocity as a function of wavelength varying from about 7,100 ft/sec (2150 m/sec) to about 8,200 ft/sec (2500 m/sec). Comparison of the dispersion curve with the cross section in Figure 6(a) shows that although some damage exists on the other side of the beam, it is not directly beneath the array; therefore, it does not affect the observed surface wave velocities. The dispersion curve indicates that intact, high-quality concrete along the plane tested in good agreement with what was predicted [Figure 7(a)].

Figures 7(b) and 7(c) indicate deep and shallow damage at arrays 18–19 and 21–22, respectively. Figure 5(a) displays an increase in the phase spectra slope for array 21–22, which is indicative of a velocity decrease. Dispersion curves in Figure 5(b) show the velocity decrease as a function of wavelength for both the 18–19 and 21–22 stations. The velocity decrease occurs at longer wavelengths with the deep damage for Array 18–19 but affects shorter wavelengths when the damage is closer to the surface for Array 21–22. Again, the SASW dispersion curves are in good agreement with the predicted cross sections.

Data from Figure 5(b) were posted with velocity data from the rest of the beam on the velocity contour plot shown in Figure 8. Trends present on the contour plot indicate how the SASW method is able to delineate damage within the beam through variations in surface wave velocity. The velocity decrease between Stations 17 and 22 corresponds to a transition zone between undamaged and damaged concrete. The low velocity zone between Stations 22 and 33 corresponds to the severely damaged portion of the beam. An increase in velocity between Stations 33 and 37 indicates another transition zone between damaged and undamaged concrete. Velocities measured beyond Station 37 return to those of undamaged concrete. However, another anomalous zone exists between Stations 45 and 49, where little or no damage is visible. In general, surface wave velocities in undamaged portions of the beam ranged between 7,100 and 9,000 ft/sec (2150 to 2750 m/sec), but were concentrated around 7,800 ft/sec (2400 m/sec). Surface wave velocities in damaged zones ranged from 4,000 to 6,900 ft/sec (1200 to 2100 m/sec).

Surface wave measurements made between Stations 17 and 22 indicate how the SASW method may be used to identify damage that is visually undetectable on the surface being tested. All wavelengths in the undamaged zone at Station 17 possessed intact concrete velocities, as shown in Figure 8, but velocities decreased as stations approached the damaged zone. The longer-wavelength velocities were the only ones to decrease initially; however, all wavelengths were affected once the stations were within the damaged zone at Station 22. Previous observations of other specimens may explain the wavelength dependence (*12,14*). Observation of concrete specimens with finite thickness reveal that velocities decrease when wavelengths exceed the concrete thickness because of interference from the concrete-air interface on the opposite side of the specimen. A large crack existed within the concrete member between Stations 17 and 22, as indicated on the cross sections in Figure 7(b) and 7(c). The crack was roughly parallel to the surface being tested, but dipped from Station 22 to 17. The crack may have acted as a concrete-air interface and caused the velocities of the wavelengths greater than its depth to decrease. The crack expressed itself on the bottom and nonimpacted side of the beam, but was visually undetectable between Stations 17 and 22 on the surface being tested.

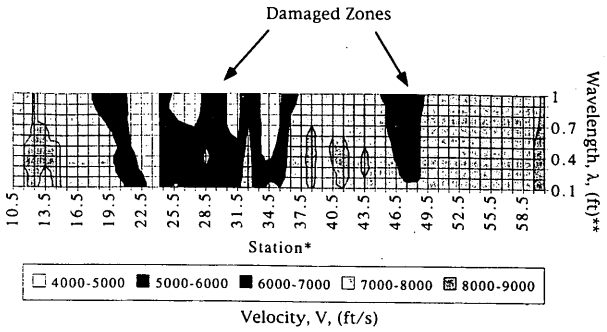

Note: *Velocities plotted midway between receiver stations; hence for Array 10-11, data is plotted at station 10.5.
**Wavelength is empirically related to depth into concrete beam.

FIGURE 8 Contoured surface wave velocity data from SASW testing of overpass beam.

Given a situation in which the bottom and nonimpacted sides of the beam are not accessible for visual inspection, SASW testing could be used as an indicator of otherwise invisible damage within the beam. The depth to the crack also could be estimated as the point on the dispersion curve where the velocities of increasing wavelengths begin to decrease.

Surface wave measurements taken between Stations 33 and 37 also demonstrate the potential of the SASW method to delineate internal damage. The transition zone between damaged and undamaged concrete is indicated by an increase in surface wave velocity from Stations 33 to 37. A crack crosses the array axis in the "undamaged" zone at Station 42, but the crack is apparently not significant enough to decrease surface wave velocity. The crack may be superficial enough not to affect surface wave propagation, or it may possess acoustic "bridges" of undamaged material that allow the surface wave energy to cross. At any rate, there seems to be a threshold crack area below which surface wave velocities are not affected. Future work to compare SASW-detectable cracking with strength-reducing cracking should address the significance of this finding by determining how much of the strength-reducing damage SASW testing can detect.

Measurements taken between Stations 45 and 49 demonstrated the potential of the SASW method to delineate internal damage. The surface wave velocities measured in this interval appear to indicate internal damage caused by bulging of the beam when it was struck. This damage is suggested by the presence of cracking near Stations 45 through 49, but the SASW velocity information delineates specific zones of damage. The velocity decrease with increasing wavelength may indicate damaged concrete overlain by undamaged concrete, but it also may indicate an internal delamination-type crack parallel to the surface being tested. This crack could be acting as a free surface that decreases the longer-wavelength velocities similar to the Station 17–22 interval. In either case, the surface wave velocity decrease in the Station 45–49 interval indicates internal damage within the beam that may not have been predicted solely on the basis of visual inspection.

CONCLUSIONS

The results of this study demonstrate the qualitative ability of the SASW method to confirm and delineate internal cracking within a

damaged concrete structural element. Surface wave velocities in the undamaged portions of the overpass beam used in this study ranged between 7,100 and 9,000 ft/sec (2150 and 2750 m/sec), but were concentrated around 7,800 ft/sec (2400 m/sec). Surface wave velocities in damaged zones ranged from 4,000 to 6,900 ft/sec (1200 to 2100 m/sec). These slow velocity zones indicated internal damage between Stations 18 and 37 and again between Stations 45 and 49. The velocity contrasts along the beam corresponded well with the external cracking present on the beam and fairly well with the internal damage estimated on the cross sections. Visual inspection of the cross-sections alone supported only a crude interpretation of the internal damage. However, surface wave velocity information provided by the SASW method suggests that SASW testing can be used to confirm and delineate the internal damage initially predicted upon visual inspection. As importantly, this testing could be used to determine whether damaged zones had been repaired adequately by epoxy grouting for instance, once a repair operation is complete. A poor grout job presumably would leave voids in the concrete that could be identified by SASW testing as slow-velocity zones.

Note, however, that a velocity decrease at a given wavelength does not necessarily mean the concrete is damaged at depths greater than that wavelength. The behavior of a surface wave with a given wavelength is dominated by the material between the surface and a depth equal to about one-third of the wavelength. That holds for all surface waves, regardless of the crack geometry.

Forward modeling or inversion is the process that uses dispersion curve data to create a profile of shear wave velocity or modulus versus depth. Inversion theory for layered systems generally is based on assumptions of a continuous system possessing vertical stiffness gradients. However, a system such as cracked concrete is more complex. Cracks act as discontinuities between pieces of concrete that otherwise would be relatively homogeneous and isotropic. Future work should be aimed at understanding the more complicated systems and the mechanisms that cause surface wave velocities to decrease, before an appropriate inversion method can be developed.

Even with the quantification of surface wave data through accurate inversion, the SASW method will have limitations. Cracks resealed by an applied force, such as a bending force or a prestressed tendon, cannot be detected (*14*). Cracks existing on the opposite side of a concrete specimen from the SASW array are undetectable if they are less than half the thickness of the specimen. However, such cracks would be detected if other sides of the beam were accessible for SASW testing. This could greatly increase the volume of data to be manipulated. Further work needs to be aimed at streamlining data acquisition and processing methods to manage efficiently the larger volumes of data.

ACKNOWLEDGMENTS

The authors thank Riyad Aboutaha, Rob Zobel, and the other researchers and staff at Ferguson Structural Engineering Laboratory of the University of Texas at Austin. Their cooperation in allowing collection of data on their specimens is greatly appreciated. The authors also thank the Texas Department of Transportation for providing support for two projects under the technical guidance of Jeff Jackson and Robert Cochrane. Finally, support from the National Science Foundation is greatly appreciated.

REFERENCES

1. Ballard, R. F., Jr. *Determination of Soil Shear Moduli at Depth by In Situ Vibratory Techniques.* Miscellaneous Paper No. 4-691, U.S. Army Corps of Engineers Waterways Experiment Station, Vicksburg, Miss., 1964.
2. Heukelom, W., and C. R. Foster. Dynamic Testing of Pavements. *Proc., ASCE Journal of Soil Mechanics and Foundations Division,* Vol. 86, No. SM1, Part 1, Feb., 1960.
3. Richart, F. E., Jr., J. R. Hall, Jr., and R. D. Woods. *Vibrations of Soils and Foundations.* Prentice Hall, Englewood Cliffs, N.J., 1970.
4. Stokoe, K. H., II, G. J. Rix, and S. Nazarian. In Situ Seismic Testing with Surface Waves. *Proc., 12th International Conference on Soil Mechanics and Foundation Engineering,* Rio de Janeiro. Brazil, 1989.
5. Stokoe, K. H., II, S. Nazarian, G. J. Rix, I. Sanchez-Salinero, J. C. Sheu, and Y. J. Mok. In Situ Seismic Testing of Hard-to-Sample Soils by Surface Wave Method. *Proc., 40th Geotechnical Engineering Conference,* University of Minnesota at Minneapolis, 1992.
6. Nazarian, S., K. H. Stokoe, II, R. C. Briggs, and R. Rogers. Determination of Pavement Layer Thicknesses and Moduli by SASW Method. In *Transportation Research Record No. 1196,* TRB, National Research Council, Washington, D. C., 1988, pp. 133–150.
7. Nazarian, S. *In Situ Determination of Elastic Moduli of Soil Deposits and Pavement Systems by Spectral-Analysis-of-Surface-Waves Method.* Ph.D. dissertation. University of Texas at Austin, 1984.
8. Sanchez-Salinero, I. *Analytical Investigation of Seismic Methods Used for Engineering Applications.* Ph.D. dissertation. University of Texas at Austin, 1987.
9. Bay, J. A., and K. H. Stokoe II. Field Determination of Stiffness and Integrity of PCC Slabs Using the SASW Method. *Proc., Conference on Nondestructive Evaluation of Civil Structures and Materials,* University of Colorado at Boulder, 1990.
10. Roesset, J. M., D. W. Chang, and K. H. Stokoe II. Comparison of 2-D and 3-D Models for Analysis of Surface Wave Tests. *Proc., 5th International Conference on Soil Dynamics and Earthquake Engineering,* Karlsruhe, Germany, 1991, pp. 11–26.
11. Foinquinos Mera, R. *Analytical Study and Inversion for the Spectral Analysis of Surface Waves Method.* M. S. thesis. University of Texas at Austin, 1991.
12. Bowen, B. R. *Damage Detection in Concrete Elements with Surface Wave Measurements.* Ph.D. dissertation. University of Texas at Austin, 1992.
13. Madianos, M. *Field and Laboratory Investigation* of *Rock Masses Using Surface Wave Seismic Testing (SASW).* M. S. thesis. University of Texas at Austin, 1991.
14. Kalinski, M. E. Measurements of Internally Cracked Concrete Structural Elements by the SASW Method. M. S. thesis. University of Texas at Austin. (n.d.)
15. Achenbach, J. *Wave Propagation in Elastic Solids.* Elsevier Publishing Company, New York, 1973.

Publication of this paper sponsored by Committee on Performance of Concrete.